

Are the experimentally observed 3-dimensional Carbon honeycombs, all-sp² structures? The dangling p-orbital instability.

Electronic Supplementary Information

Zacharias G. Fthenakis

Abstract of the main manuscript: Recently, Krainyukova and Zubarev [Phys. Rev. Lett. **116**, 055501 (2016)] reported that they observed a series of all-sp² 3-dimensional Carbon honeycomb structures with interesting storage properties. In the present study we show that these structures are unstable, reducing to honeycomb structures with sp³ atoms at the honeycomb junctions. As we show, this instability is owed to the solitary electrons occupying the unhybridized *p* orbitals of the junction atoms, thus violating the octet rule. These orbitals are localized and have all the features that characterize the *dangling orbitals*. This instability, as well as the ability of unhybridized *p* orbitals to form dangling bonds has not been reported previously.

1 Structural features of structures A and B

In Tab. 1 we present the bond lengths and bond angles, as well as the lengths *a* and *c* of the unit cell vectors of structures A and B, calculated using the DFT method with the LDA/CA and the GGA/PBE functionals. For comparison between the bond lengths and the bond angles of structures A and B, the counterparts of *d*'_{*i*} bond lengths of structure B are the *d*_{*i*} bond lengths of structure A.

As we can see, the lengths of the bonds at the walls of structure A, do not differ considerably from the corresponding bond lengths of structure B. These bond length differences do not exceed the value of 0.05 Å. However, the interatomic distances of their junction atoms differ significantly (approximately 0.8 Å).

Similar picture is obtained for bond angles. Bond angles of structures A and B, formed between the junction atom bonds (i.e. the bonds with lengths *d* and *d*₁) and their neighboring bonds (i.e. bonds with lengths *d*₂ and *d*'₂) differ significantly (by approximately 12 - 16°), while the rest of the bond angles differ by less than 3.5°.

On the other hand the unit cell vector lengths *a* and *c* of structures A and B differs by less than 1%, and therefore, practically they do not change as structure A is transformed to structure B.

The conclusion therefore is that the conversion of structure A to structure B affects mainly the junctions.

2 A possible instability mechanism

In order to understand if the transition mechanism which converts structure A to structure B is similar to the mechanism converting graphite with AA stacking to hexagonal diamond under pressure¹ and is partly responsible for the instability of H-6 Car-

bon², we consider a transition path like the one described by Eqs. 1 of the main manuscript and we follow the same procedure as we did in the main manuscript.

The two ends of this transition path are (i) graphite with AA stacking and the local structural features of structure A at the junctions (initial point), and (ii) hexagonal diamond with the local structural features of structure B at the junctions (final point). Thus, the unit cell vectors, corresponding both to the initial and the final structures, have the form of Eq. 2 of the main manuscript and contain four atoms. The coordinates *r*_{*i*}, *i* = 1, 2, 3, 4, of these atoms, as well as the lengths *a* and *c* of the unit cell vectors, are shown in Tab. 2.

We calculate the energy along this transition pathway using the DFT method with the LDA/CA functional. The energy per atom as a function of the parameter *λ* of Eq. 1 of the main manuscript is shown in Fig. 1. As we can see in this figure, there is an energy barrier of ≈ 0.06 eV/atom along this transition path not allowing the spontaneous transition of graphite with AA stacking and the structural features of structure A to hexagonal diamond with the structural features of structure B. Contrary to this, the corresponding transition path, converting structure A to structure B, does not have a barrier, as shown in Fig. 2(f) of the main manuscript. Therefore, the conversion of graphite with AA stacking to hexagonal diamond is not favored in our case, and consequently, the mechanism responsible for the instability of structure A is not the same with that converting graphite with AA stacking to hexagonal diamond.

References

- 1 S. Fahy, S. G. Louie and M. L. Cohen, *Phys. Rev. B*, 1987, **35**, 7623–7626.
- 2 Z. G. Fthenakis, *RSC Adv.*, 2016, **6**, 78187–78193.

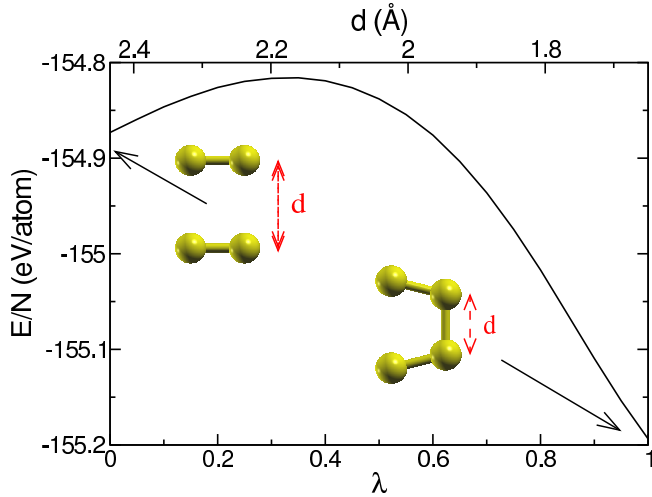


Fig. 1 Transformation path for the conversion of graphite with AA stacking and structural features of the junctions of structure A, to hexagonal diamond with structural features of the junctions of structure B. The unit cells corresponding to the two ends of the path are depicted. The opposite x-axis represents the interatomic distance d along the path.

	Structure A		Structure B	
	LDA/CA	GGA/PBE	LDA/CA	GGA/PBE
a	10.1234	10.2047	10.1049	10.1644
c	2.4345	2.4550	4.8632	4.8989
$2c$	4.8690	4.9100		
d	2.4345	2.4550	1.6499	1.6656
d'	-	-	3.2133	3.2332
d_1	1.4822	1.4965	1.5142	1.5295
d_2	1.4123	1.4225	1.3983	1.4072
d_2'	-	-	1.4182	1.4278
d_3	1.4496	1.4631	1.4074	1.4185
d_3'	-	-	1.5095	1.5232
$\widehat{(d, d_1)}$	90.000	90.000	103.925	103.795
$\widehat{(d_1, d_2)}$	120.469	120.356	107.800	107.879
$\widehat{(d_2, d_2)}$	119.061	119.328	116.553	116.648
$\widehat{(d_2, d_3)}$	120.469	120.356	121.722	121.676
$\widehat{(d', d_1)}$	-	-	76.075	76.205
$\widehat{(d_1, d_2')}$	-	-	132.768	132.533
$\widehat{(d_2, d_2')}$	-	-	119.435	119.586
$\widehat{(d_2', d_2')}$	-	-	122.313	122.524
$\widehat{(d_2', d_3')}$	-	-	118.843	118.738

Table 1 Comparison between structural features of structures A and B optimized using DFT with both LDA/CA and GGA/PBE functionals. a and c are the lengths of the unit cell vectors, d and d' are the interatomic distances between the junction atoms, d_1 , d_2 , d_2' , d_3 and d_3' are the different bond lengths of structures A and B and $\widehat{(d_i, d_j)}$ are the bond angles formed by the bonds with lengths d_i and d_j . The bonds corresponding to these bond lengths, are shown in Figs. 2(c) and (d) of the main manuscript. All lengths and angles are expressed in Å and deg units, respectively.

	Initial Structure ($\lambda = 0$)	Final Structure ($\lambda = 1$)
a	$\sqrt{3}d_{1A} = 2.5672 \text{ \AA}$	$\sqrt{3}d_{1B} \cos \phi = 2.5455 \text{ \AA}$
c	$2d_A = 4.8690 \text{ \AA}$	$2(d_B + d_{1B} \sin \phi) = 4.0286 \text{ \AA}$
\mathbf{r}_1	(0, 0, 0)	(0, 0, 0)
\mathbf{r}_2	$(d_{1A}, 0, 0)$	$(d_{1B} \cos \phi, 0, d_{1B} \sin \phi)$
\mathbf{r}_3	$(0, 0, d_A)$	$(0, 0, 2d_{1B} \sin \phi + d_B)$
\mathbf{r}_4	$(d_{1A}, 0, d_A)$	$(d_{1B} \cos \phi, 0, d_{1B} \sin \phi + d_B)$

Table 2 Lengths a and c of the unit cell vectors and coordinates \mathbf{r}_i , $i = 1, 2, 3, 4$ of the four atoms contained in the unit cell for the initial and the final structures along the transition path. d_{1A} and d_{1B} are the d_1 values for structures A and B, respectively, d_A and d_B are the d values for structures A and B, respectively, and ϕ is the angle between the bond with length d_1 and the line normal to the junction axis in structure B. The values of d_{1A} , d_{1B} , d_A and d_B are shown in Tab. 1, while $\phi = (\widehat{(d, d_1)} - 90^\circ) = 13.925^\circ$ (for the LDA/CA calculation).